Hindawi
Advances in Materials Science and Engineering
Volume 2023, Article ID 9857328, 1 page
https://doi.org/10.1155/2023/9857328

Retraction

Retracted: Predicting the Elastic Modulus of Nanoparticle-Reinforced Polymer Matrix Composites Based on Digital Image Processing and Finite Elements

Advances in Materials Science and Engineering

Received 26 December 2023; Accepted 26 December 2023; Published 29 December 2023

This article has been retracted by Hindawi, as publisher, following an investigation undertaken by the publisher [1]. This investigation has uncovered evidence of systematic manipulation of the publication and peer-review process. We cannot, therefore, vouch for the reliability or integrity of this article.

Please note that this notice is intended solely to alert readers that the peer-review process of this article has been compromised.

Wiley and Hindawi regret that the usual quality checks did not identify these issues before publication and have since put additional measures in place to safeguard research integrity.

We wish to credit our Research Integrity and Research Publishing teams and anonymous and named external researchers and research integrity experts for contributing to this investigation.

The corresponding author, as the representative of all authors, has been given the opportunity to register their agreement or disagreement to this retraction. We have kept a record of any response received.

References

[1] Z. Jiang and C. Zhou, "Predicting the Elastic Modulus of Nanoparticle-Reinforced Polymer Matrix Composites Based on Digital Image Processing and Finite Elements," *Advances in Materials Science and Engineering*, vol. 2022, Article ID 7884623, 12 pages, 2022.

Hindawi
Advances in Materials Science and Engineering
Volume 2022, Article ID 7884623, 12 pages
https://doi.org/10.1155/2022/7884623

Research Article

Predicting the Elastic Modulus of Nanoparticle-Reinforced Polymer Matrix Composites Based on Digital Image Processing and Finite Elements

Zhenghong Jiang[1] **and Chunrong Zhou**[2]

[1]*School of Big Data, Chongqing Vocational College of Transportation, Jiangjin 402260, Chongqing, China*
[2]*Science and Technology Branch, Chongqing Vocational College of Transportation, Jiangjin 402260, Chongqing, China*

Correspondence should be addressed to Zhenghong Jiang; jiangzhenghong@cqjy.edu.cn

Received 13 May 2022; Revised 21 June 2022; Accepted 29 June 2022; Published 21 July 2022

Academic Editor: Haichang Zhang

"Composite" means composition of two or more separate components. Composites are materials composed of two or more components that are chemically separated from each other on a macroscopic scale, and there are interfaces between these components. Conceptually, fiber-reinforced composites have existed since about 800 B.C. The aim of this paper is to predict the elastic modulus of nanoparticle-reinforced polymer matrix composites based on digital image processing and finite elements and to investigate the presence of interfaces in three-phase particle-reinforced composites. In this paper, the interfacial layer is designed as a spring model with the help of the effective modulus law, a statistical debonding criterion is proposed to represent the proceeding changes, and metallurgical methods are used to optimize the particles and prepare different composites with uniform dispersion. The experimental results of this paper show that the highest increase in tensile strength of the composites is about 8% and the highest increase in elastic modulus is 40% after the addition of nanoparticle materials, and the highest increase in tensile strength is 18% and the highest increase in elastic modulus is 50% after the addition of CNFs.

1. Introduction

1.1. Background. With the continuous progress of science and technology, polymer materials are more and more widely used in daily life, along with the high demand on the performance of polymer materials, knowing that the emergence of nanopolymers only solved the real problem. Particle-reinforced composites have superiority that cannot be matched by other materials and can be seen in many fields. At present, nanoparticle-reinforced polymer-based composites are one of the research hotspots in the field of science. The composite material has the characteristics of high specific strength, high specific modulus, high fatigue resistance, strong fracture resistance, good high-temperature performance, and strong creep resistance. However, due to the characteristics of nanoparticles indicating a high number of atoms and high activity, the effectiveness of nanomaterials themselves cannot be utilized [1]. With the advancement of science and technology, digital image processing technology has been developed rapidly, and researchers believe that it is expected to use digital image processing technology to start the research on nanomaterials and solve the current dilemma faced.

1.2. Significance. The use of nanomaterials to enhance polymer-based composites can improve the dispersion of nanomaterials, so that they are more uniformly distributed in the matrix and play the effect they have and, at the same time, can improve the surface activity of the particles, enhance the association with the matrix, get the performance of different materials, and enhance the compatibility of the rest of the polymer before leaching [2].

1.3. Related Work. In the present, there are many ways to modify the properties of materials, but most of them are derived from experimental data, which do not allow an accurate characterization of the properties of composite, and this method is not easy to operate, so researchers started to start in other ways. Barbedo proposed a new computer algorithm to distinguish the signs and symptoms of plant diseases from the asymptomatic tissue in plant leaves. The simple algorithm processes histograms of the H (from the HSV color space) and a (from the L ∗ a∗ b∗ color space) color channels. All steps in the algorithm process are automatic, except for the final step where the user decides which channel (H or a) provides better discrimination. The disease discrimination problem is analyzed in depth, and the problems of lesion delimitation, lighting, leaf vein interference, and leaf roughness are discussed in depth. The proposed algorithm was tested under a variety of conditions, including 19 plants, 82 diseases, and images collected under controlled and uncontrolled environmental conditions. The algorithm proved to be applicable to a wide range of plant diseases and conditions, although some situations may require other solutions [3]. Stachiv proposed an easily accessible resonance-based method that can simultaneously determine the residual stress, elastic modulus, density, and thickness of ultra-thin films coated on dual-clamped micro/nanobeams. Film is a type of composite material. The general dependence of the resonance frequency on the axial load also applies to in-plane vibrations and depends only on the vibration mode under consideration. It was found that the elastic modulus, density, and thickness of the film can be evaluated by the two measured in-plane and out-of-plane fundamental resonance frequencies of micro/nanobeams with and without film under different prestresses. However, the residual stress can be determined from the continuous resonant frequencies of the beam and the film under different prestresses measured outside the two planes (in-plane) without knowing the characteristics and dimensions of the film and the substrate. It also reveals that the common uncertainties in the force (and thickness) determination have negligible influence on the determined film properties [4]. Hawileh presented an experimental program that investigates the mechanical properties of carbon (C), basalt (B), and their multilayer hybrid combinations (BC, CBC, CCB, BBC, and BCB) at high temperatures. The experimental procedure consisted of 140 specimens prepared and tested after exposure to different temperatures ranging from 25 to 250 °C. The results showed that the modulus of elasticity and tensile strength of C and B laminates decreased with increasing temperature. The lack of knowledge about the mechanical properties of such laminates and their hybrid combinations was filled [5]. Nedeljkovic investigated the effect of natural carbonation on the pore structure and elastic modulus (Em) of alkali-activated fly ash (FA) and ground granulated blast furnace slag (GBFS) pastes after one year of exposure to the environment. Chemical changes due to carbonation were detected by X-ray diffraction (XRD), scanning electron microscopy/energy dispersive X-ray (SEM-EDX), and attenuated total reflection Fourier transform infrared spectroscopy (ATR-FTIR). Subsequently, the pore structure and Em of the degraded materials were tested by mercury-in-pressure (MIP), nitrogen (N-2) adsorption, and nanoindentation. Chemical degradation of alkali-activated pastes due to natural carbonation was shown to depend on the GBFS content and the development of its pore structure. The pure alkali-activated GBFS pastes were found not to be carbonated at all during the test period due to the fine gel pore structure [6]. Xu designed an n-phase micromechanical framework to predict the effective thermal conductivity and elastic modulus of multicomponent particulate composites consisting of hard and soft anisotropic shaped inclusions, their surrounding weak interfaces, and the matrix. In this micromechanical model, the volume fractions of the weak interfaces treated as interface models are quantified and merged into the n-phase differential effective medium model. The results show that the structural configuration of the interfaces has a significant effect on the effective physical-mechanical properties of the particulate composites. The effective conductivity and elastic modulus of the multicomponent particle composites were well predicted by the micromechanical model through comp [7]. Wei studied the hardness and elastic modulus of Ag/Nb multilayers with monolayer thickness (T) ranging from 1 to 50 nm. The hardness increased with decreasing h, and the hardness values of multilayers with $h \leq 5$ nm were higher than those of either component. This ultra-high strength arises from the coherent stress in the Ag layer and the high density stacking layer fault. Also, when $h \leq 20$ nm, an increase in elastic modulus is achieved due to lattice shrinkage, where the modulus values are higher than those of either component, exhibiting a supermodulus effect [8]. Xin proposed a numerical method combining the discrete element method and digital image processing. The actual inhomogeneity of the rock is captured by digital image processing (DIP) and used as input to build a numerical discrete element model. The contact between mineral grains is established by finding the boundaries of the different mineral compositions. The microscopic damage process is investigated by numerical simulations of Brazilian tests on granite samples. Discrete element is a numerical simulation method specially used to solve the problem of discontinuous medium. This method regards the jointed rock mass as composed of discrete rock blocks and joint surfaces between the rock blocks, allowing the rock blocks to translate, rotate, and deform. The joint surfaces can be compressed, separated, or slipped. Numerical results show that crack sprouting is strongly influenced by the actual spatial distribution of mineral grains and that the crack sprouting and extension processes may differ significantly from the actual spatial distribution of mineral grains due to inhomogeneities [9]. Xia proposed a new method for screening mold strains by applying image processing and support vector machines (SVMs). As an example, the morphological characteristics of red *Aspergillus* colonies were quantified by image processing. And the association between features and pigment productivity is determined by SVMs. Based on this, a highly automated screening strategy was implemented. The accuracy of the proposed strategy was 80.6%, which is compatible with existing methods (81.1% for microplates and 85.4% for

flasks). Also, the screening of 500 colonies took only 20–30 min, the fastest of all published results. By applying this automated method, 13 strains with high predicted yields were obtained, with the best strains being 2.8 times more pigmented (226 U/mL) and 1.9 times more lovastatin (51 mg/L) compared with the parental strains. The current study provides us with an effective and promising method for strain improvement [10]. Although these theories have been investigated to some extent for polymer matrix composites, the methods used are too complex for practical use.

1.4. Innovation Points. An effective modulus prediction scheme for particle-reinforced composites based on the effective strain theory of the energy method is proposed. Compared with the previous volume-averaged strain to represent the effective strain of the composite as a whole, the effective strain method based on the energy method can reflect the energy reserves present in the particle-reinforced composite more realistically, and the two interface cases where the interface surrounding the particle inclusions is a hard interface material or a soft interface material are taken into account.

2. Prediction of Elastic Modulus of Nanoparticle-Reinforced Polymer Matrix Composites Based on Digital Image Processing and Finite Element Method

2.1. Digital Image Processing. Digital image processing is also known as computer image processing. Conceptually, a digital image consists of pixels, which are the basic units of an image. Digital image processing targets digital images, which simply means that the information on the target image is converted into the corresponding digital information, and then the obtained information is subjected to arithmetic, that is, the information obtained from the target image is smoothed, noise reduction or compression, and we collectively refer to this technique as digital image processing in academic terms [11]. Figure 1 illustrates the framework of digital image processing.

According to research findings, the vast majority of the information obtained in human daily life originates from vision. Information sources also include senses such as touch and hearing. Compared with other information, images provide richer and more accurate information and are used very frequently in practice because of their more comprehensive functions; in fact, digital image processing techniques are used once information within the visual domain is studied [12, 13].

Digital image processing techniques contain a very basic function [14]. It is the enhancement of digital image information. This takes up a very large space for images without any intervention, and the processing is very complex, so it is necessary to convert the target image in the spatial or frequency domain before formal processing. The space domain consists of image pixels, and the frequency domain describes the frequency structure of the signal and the relationship between the frequency and the amplitude of the frequency signal. Image compression techniques are often used in this process. Restoration or enhancement of the target image is performed to enhance some aspect of the information features of the target image; segmentation techniques are used to extract the information that needs to be utilized in the target image [15, 16]. At this stage, a simple description of the target image is often used to describe a two-dimensional image, after which a category analysis of the target image information is required [17]. The two-dimensional image description is not easy to change due to noise and other original columns and has the ability to distinguish similar objects. After a series of processing, whether the image is pasted, copied, stored, or cut, no damage is caused in the image itself, but analog images before the advent of digital imaging technology could not achieve such functionality. Therefore, in practical applications, digital image processing technology is widely used in various fields and can be combined with mathematical calculations to process relevant images more flexibly [18]. Figure 2 shows a schematic diagram of digital image processing.

Digital graphics processing technology dates back to the early 1920s, when it was first applied to improve the quality of the images transmitted over the submarine cable between London and New York, thanks to the development of computer technology at that time, which allowed the combination of computer technology with image-related information. It was not until the booming of the third technological revolution, which led to the take-off of computer technology, that digital image processing techniques gained increasing attention [19]. In the middle of the last century, digital image processing technology began to improve its branches, and its own processing technology slowly became sound and began to emerge as an emerging discipline [20]. At this stage, digital image processing technology was mainly applied to text recognition and medical image processing until the end of the development of the last century, when digital image processing technology began as an independent disciplinary technology. Due to the continuous development of modern science and technology, the requirements for digital image processing have become more stringent, which has forced the continuous development of digital image processing technology, especially in computer image vision, which has achieved the development of two-dimensional images wanting 3D [21]. This technology makes the image detail processing more perfect, and the information obtained after the processing of the target image gives more obvious perception and more outstanding effect. In short, the process of digital image processing is to input an image with poor quality and inconspicuous details, and then its output image is a high-quality image that can highlight the required details. The common processing methods include image smoothing and compression coding [22].

Due to the deep development of computer technology in recent years, the extensive use of mathematical knowledge has led to the development of digital image processing, and in recent years, due to the increased demand for agriculture,

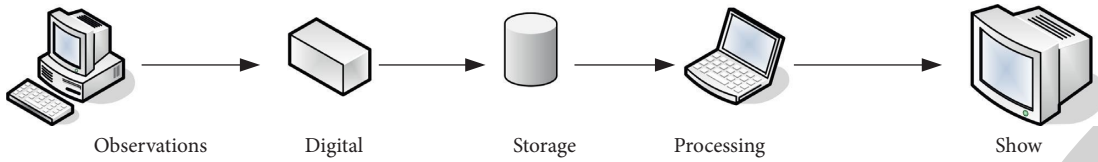

Figure 1: Framework diagram of digital image processing.

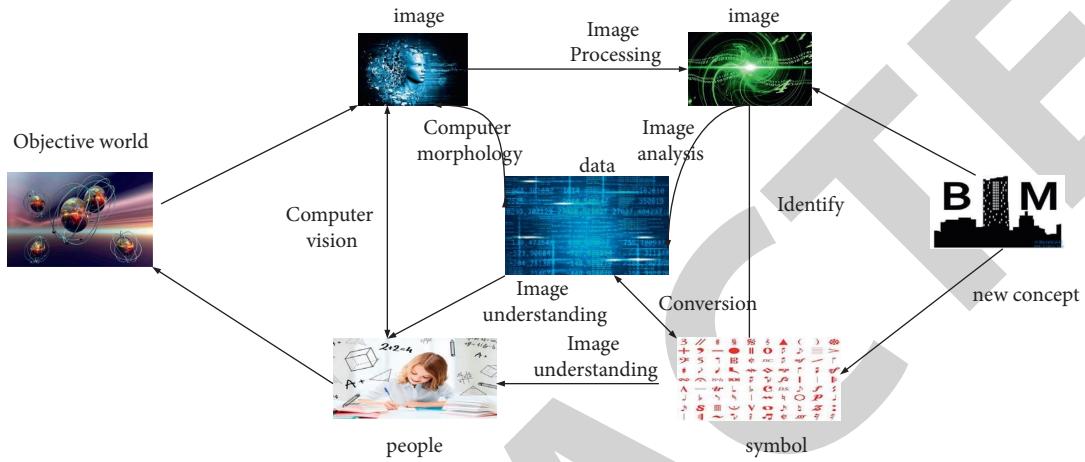

Figure 2: Schematic diagram of digital image processing.

forestry, animal husbandry and fishery, aerospace, military, and medical technology, all of which continue to push the development of digital image technology [23]. At present, the development of digital processing technology can be described from three aspects, including traditional technology, image-to-technology, and data-to-image; with the continuous development of technology, it contains more and more areas, due to the continuous development and improvement of each field of its own technology, so the requirements of digital image processing technology are becoming more and more stringent, requiring traditional technology for the experimentation of new technology to continuously improve [24].

The first category belongs to the image-to-image. That is, the input image and the output image, the compression coding and recovery of the image are derived from this technique. In fact, in the image processing process, the image quality is compromised due to many factors, which makes the target image unrecognizable in terms of what needs to be highlighted for study. In order to highlight the features that need to be studied or are of interest in the image, and to attenuate the unimportant information so that the image is easier to read and suitable for human eyes to observe and analyze, enhancement techniques are used, such as denoise the image, enhance the contrast, sharpen or blur the image, and convert grayscale and RGB images [25, 26]. Figure 3 shows the image conversion schematic.

In fact image restoration techniques can also restore the quality of the target image to some extent, the principle applied by this method is to remove the noise and blurred edges of the image or to use timely enhancement to get the original image [27]. Figure 4 shows a schematic representation of the data processing structure.

The second category is image-to-technology, which in short means that the input is an image, but the output is a symbol, and the symbolic information is used to represent the target image information [28]. For example, information about medical images is tagged so that the input image can be used to understand the patient's physical condition. Image recognition techniques need to be applied in this type of digital image processing. In the target image segmentation process, the target image is first superimposed and the segmentation can be classified according to the image, color, or other indicators. In practice, we need to categorize the grayscale values of the target images beforehand and only after that we can process them separately [29].

The third category is data-to-image type. In layman's terms, this belongs to the image reconstruction process, which is the inverse process of processing the target image by employing quantization. Through this technique, images with certain characteristics can be created using relevant data, and these techniques are widely used within the field of scanning [30].

2.2. Digital Image Computation. The core principle of histogram equalization is to make changes in the number of pixels to improve the pixel contrast, and the expression of the transformation function is shown as follows:

$$l = W(a), 0 \le a \le r - 1, \tag{1}$$

where a represents the grayscale of the image processing; when the value of a represents zero, it means that the color of d is black at this time.

$W(a)$ is a continuous differentiable function for which the following expression can be obtained after a brief transformation:

Figure 3: Schematic diagram of image conversion.

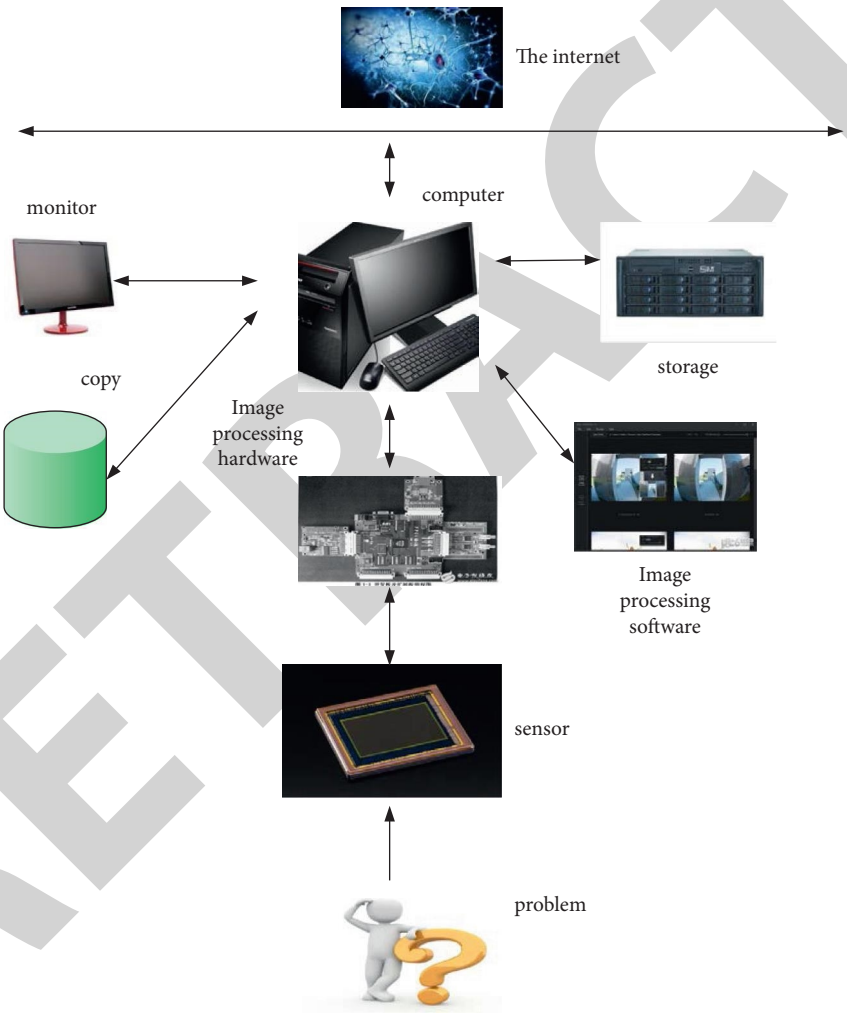

Figure 4: Data processing structure diagram.

$$q_i(i) = q_w(w)\left|\frac{\mathrm{d}w}{\mathrm{d}i}\right|. \tag{2}$$

In the above equation, the grayscale variable i is determined by the PDF of the input grayscale and the transform function used.

The commonly used transformations in image processing are shown as follows:

$$I = W(a) = (R-1)\int_0^a q_a(s)\mathrm{d}s, \tag{3}$$

where s represents the dummy variable of the integral and R denotes the range of values taken.

Then, according to the Leibniz criterion, it can be introduced that

$$\frac{\mathrm{d}i}{\mathrm{d}w} = \frac{\mathrm{d}U(w)}{\mathrm{d}w} = (R-1)\frac{d}{dw}\left[\int_0^a q_w(s)\mathrm{d}s\right] = (R-1)q_w(w). \quad (4)$$

A box of uniform PDFs can be obtained when the probability density is positive at

$$\begin{aligned} q_i(i) &= q_w(w)\left|\frac{\mathrm{d}w}{\mathrm{d}i}\right| = q_w\left|\frac{1}{(R-1)q_w(w)}\right| \\ &= \frac{1}{R-1}, 0 \le i \le R-1. \end{aligned} \quad (5)$$

For the discrete values, we directly process the probability and summation, and the formula for the transformation is shown as follows:

$$\begin{aligned} I_c = U(w_c) &= (R-1)\sum_{j=0}^{c} q_w(w_j) \\ &= \frac{(R-1)}{MN}\sum_{j=0}^{c} n_j, c = 0, 1, 2\cdots R-1. \end{aligned} \quad (6)$$

Among them, we habitually call $U(w_c)$ histogram linear transformation.

In practice, we will sample and quantize the target image, and the processing expression can be shown as follows:

$$\begin{aligned} U &= i, \\ W &= 2^e. \end{aligned} \quad (7)$$

In the above expression, U represents the sample value of the target image and W represents the grayscale value of the target image.

In a computer, the target image can be stored using binary, and the expression is shown as follows:

$$Y = \log\left(2^e\right)^{u*u} = u*u*e\,(\text{bit}). \quad (8)$$

In the above equation, y denotes the target image storage and u denotes the target image adoption value.

Inevitably, we encounter environmental factors interfering in the image processing process, which we call noise in academic terms and can be divided into two main categories according to their relationship with the image: additive noise and multiplicative noise. We denote the noise that has no effect on the image uniformly as

$$g(a,b) = y(a,b) + i(a,b). \quad (9)$$

The noise that has an effect on the image is expressed uniformly as

$$g(a,b) = y(a,b) + i(a,b)y(a,b), \quad (10)$$

where $y(a,b)$ represents the image signal and $g(a,b)$ represents the noise containing the image.

$$\begin{aligned} y(a,b) &= c, 0 \le g(a,b) < z, \\ y(a,b) &= \frac{f-z}{u-p} * g(a,b) + z, p \le g(a,b) < u, \\ y(a,b) &= f, u \le g(a,b) < mg, \end{aligned} \quad (11)$$

where the target image has grayscale values between p and u, and after extending it, its range becomes z–f, and mg is the maximum value of $g(a,b)$.

Nonsegmented functions are very common in image processing, including exponential and logarithmic functions, which can be transformed in the use of logarithmic and exponential functions with the following function expressions:

$$y(a,b) = p + \frac{\mathrm{Ln}[g(a,b)]+1}{i*Lnz} \quad (12)$$

where p, i, and z represent the slope of the curve coordinates, which can be utilized when the image needs to be processed to extend the grayscale interval. The expression of its exponential transformation is shown as follows:

$$y(a,b) = i^{z[g(a,b)-p]} - 1. \quad (13)$$

Median filtering is a common method for image processing, which mainly removes noise from images and is classified as nonlinear signal processing [31]. Median filtering is equivalent in principle to taking the median, which is taken to deal with isolated noise points, and its expression is shown below:

$$y(a,b) = me\,d\{g(a-u, b-j), (u, j \in Q)\}. \quad (14)$$

2.3. Nanoparticles. Since the interview of carbon fiber in 1959, it has become one of the widely used materials for composite materials because of its excellent characteristics such as high strength and high modulus, and it is widely used in the field of structural materials and high-temperature materials and has the effect that other materials cannot be compared. Carbon fiber composites have high strength, good heat resistance, excellent corrosion and radiation resistance, and outstanding thermal shock resistance. With the development of nanotechnology, researchers have applied nanotechnology to composite materials, specifically to carbon fibers, making them into new nano-reinforced materials, which play a pivotal role in the modification of polymer-based materials, which have the advantages of two polymer materials in terms of specific efficacy, so nanocomposites with special performance materials [32]. As new and with great potential, composite materials have a wide range of application prospects in various sectors of society and have become a current research hotspot. Figure 5 shows the microscopic schematic of carbon nanofibers.

The dispersion state of the nano-nanofillers and the interfacial interaction with the polymer matrix are the key factors affecting the properties of the composites. However, the GO surface contains a large number of hydrophilic groups, which would be detrimental to its direct dispersion in the polymer matrix. GO denotes graphene oxide and is expected to achieve the desired effect of light weight and high specific strength. Some early researchers have found that the addition of unmodified GO has far from the expected improvement of polymer properties. In order to promote the dispersion of GO and improve the interfacial

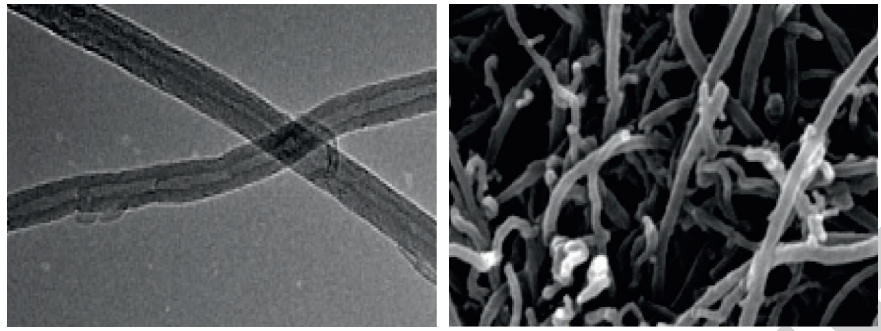

Figure 5: Microscope schematic of carbon nanofibers.

interaction with the polymer matrix, pretreatment of the GO lamellar surface is required. Surface functionalization modification of nanofillers is an effective way to improve the interfacial interaction with the polymer matrix and to promote dispersion in the polymer matrix. The GO surface contains a large number of reactive groups, which can be modified by surface functionalization to promote its dispersion in the polymer matrix and to improve the interaction with the polymer matrix. Amination modification of GO can effectively modify the composite material. In this paper, the modified GO products were obtained by pretreating the GO lamellae with KH550 silane coupling agent (KH550) and polyethyleneimine (PEI), respectively, and named as KH550GO and PEIGO.

Nanomaterials are considered to be one of the most promising materials in the 21st century, with many unique properties, which can be used to prepare excellent composite materials by introducing nanoparticles into organic polymer materials. Since then, nanocomposites have attracted a lot of attention, and various new nanomaterials and modified nanomaterials have been applied to the modification of polymer materials to produce a variety of composite materials with excellent properties. Generally speaking, nanoparticles with one-dimensional structure are more conducive to the adhesion and crystallization of molecular chains to improve crystallinity, and nanoparticles with two-dimensional structure are equivalent to a flat protective layer, which is more conducive to the improvement of barrier properties. As for the orientation system of composites, the one-dimensional nanoparticles are more easily oriented and the oriented nanoparticles are more favorable for the orientation of polymer molecular chains.

The dispersion of nanoparticles and the interfacial interaction with the polymer matrix are important factors affecting the performance of composite materials. Nanoparticles have many excellent properties and play an important role in improving the performance of polymer materials. However, when nanoparticles exist in polymer matrix in the form of agglomerates, not only can the excellent properties of nanoparticles not be played, but even become defects in the matrix, so that the dispersion of nanoparticles is an important factor affecting the performance of composite materials. The interfacial interaction between nanoparticles and polymer matrix is also an important factor affecting the performance of composite materials. The surface properties of nanoparticles are not the same, and the compatibility with polymer matrix also differs. The surface of some nanoparticles is hydrophilic and oleophobic, and it is difficult to directly disperse in organic polymer materials. The interface interaction between some nanoparticles and the matrix is weak, and the two do not have a synergistic effect, which is not conducive to the improvement of composite material performance.

3. Experiments on Predicting the Elastic Modulus of Nanoparticle-Reinforced Polymer Matrix Composites Based on Digital Image Processing and Finite Elements

3.1. Experimental Material Parameters. Materials are the material basis for human survival and the symbol of human material civilization. Materials are the pillars of modern technology, and at the same time, the progress of technology has put forward higher requirements for materials. The polymer matrix composites explored in this paper are highly designable and bring unlimited possibilities for development [33]. The material parameters involved in this paper are as follows.

As can be seen from the data in Table 1, assuming that the diameter of nanoparticles is 10 nm and the interfacial thickness layer is 10 nm, when the volume of nanoparticles keeps increasing, the elastic modulus of composites will also change and show a certain linear law, but when the diameter of particles increases, its elastic modulus will decrease and the change trend will be relatively flat.

According to the data in Table 2, it can be seen that there are many factors that affect the composite material, and the experiments were applied to each anisotropic material, but according to the data in the table, there are many materials whose values can be seen as zero, and there are also many materials whose values are closer under certain conditions. In fact, when determining the variation range of particles, the number of atoms will increase at a certain rate. When the volume fraction of nanoparticles is 6%, the number of unit cells will increase sharply, and the number of filled molecular chains will also increase rapidly.

3.2. Interaction Energy between Material and Matrix. Nanocomposites have filled particles, polymer matrix, and the interface between them. In order to explore the relationship between the properties and energy of the

Table 1: Mechanical parameters of composite materials.

Grain size	Volumetric fraction 6%			Volumetric fraction 10%		
	A (GPa)	B (GPa)	c	A (GPa)	B (GPa)	c
10	4.52	1.68	0.32	5.23	1.93	0.35
11.3	4.47	1.65	0.31	5.22	1.9	0.35
12.4	4.45	1.65	0.32	5.2	1.87	0.33
13.24	4.43	1.63	0.32	5.17	1.85	0.34
14.8	4.4	1.61	0.31	5.13	1.83	0.33

Table 2: Nanoparticle unit cell elastic stiffness matrix.

Z (GPa)	1	2	3	4	5
1	6.98	5.32	5.01	−0.31	−0.05
2	7.63	6.31	5.21	−0.04	1.37
3	6.31	4.74	6.97	1.43	0.39
4	5.02	5.25	3.28	0.41	1.39
5	−0.41	−0.03	−0.15	0.039	0.52

Table 3: Matrix action energy.

Grain size	Volume	Energy is 5%	Energy is 10%	5% energy per unit volume	10% energy per unit volume
10	4258	−304	−402	−0.09	−0.015
11.27	6512	−501	−456	−0.08	−0.06
12.3	7365	−536	−526	−0.07	−0.03
13.2	8964	−648	−614	0.06	−0.054
14.1	10,254	−712	−715	−0.043	0.048

Table 4: Single cell model and single cell mechanical properties.

Performance	PI	Volumetric fraction 5%	Volumetric fraction 10%
Young's modulus	4.15	4.6	4.79
Volume	5.4	5.87	7.43
Lamé constant	4.62	4.71	6.25
Shear modulus	1.53	1.63	1.71
Poisson's ratio	0.35	0.36	0.37

composites, single point energy calculation is needed to obtain the interaction energy between them.

According to the data in Table 3, when the execution of the nanoparticles embedded in the cell increases, the number of atoms around it also increases, and the number of nonbonding pairs between the nanoparticles and the matrix also increases, so the interaction between them also increases. Also, the qualitative correlation between the elastic properties and the interaction energy is related to the volume of the nanoparticles, when the diameter of the nanoparticles is increasing, the body surface ratio then decreases, leading to a decrease in the number of nonbonding pairs, weakening the interaction energy and leading to a decrease in the elastic modulus of the composite [34].

3.3. Single Cell Model and Single Cell Mechanical Properties. Combined with molecular dynamics, this experiment simulates the mechanical properties of the composites to explore the effect of nanoparticles and volume and to explore the correlation between the number of nanoparticles and the properties of the composites.

According to the data in Table 4, it can be seen that when nanoparticles are added to the material, Young's modulus, shear modulus, Lamé constant, and volume of the composites increase, and the data show that the difference becomes more and more obvious with the increasing volume, but the difference in Poisson's ratio change is not significant.

4. Elastic Modulus of Nanoparticle-Reinforced Polymer Matrix Composites Based on Digital Image Processing and Finite Element Prediction

4.1. Analysis of Composite Properties. According to Figure 6, it can be seen that the tensile strength, elongation, and Young's scale of the original composites are reduced to varying degrees, mainly due to the structural defects triggered by the agglomerates in the matrix, leading to a decrease in the

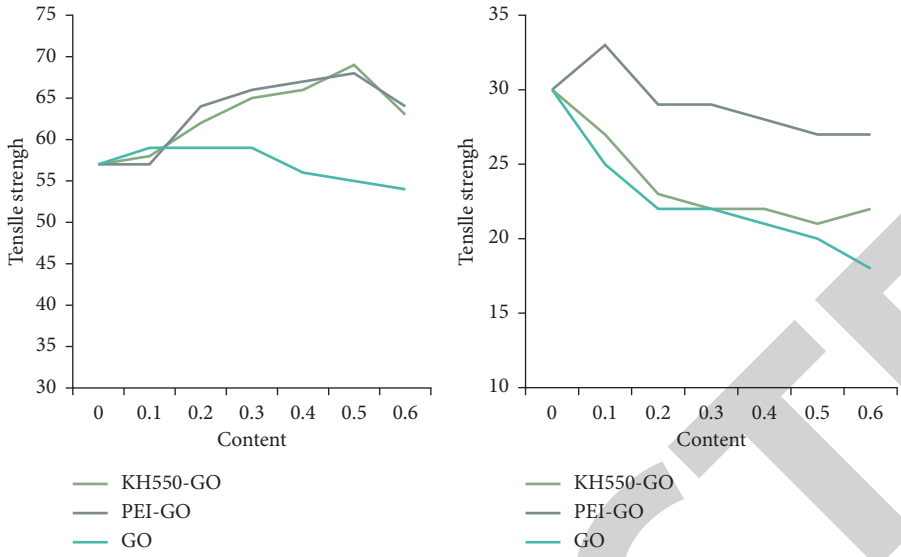

Figure 6: Schematic diagram of the secondary mechanical properties of the composite material.

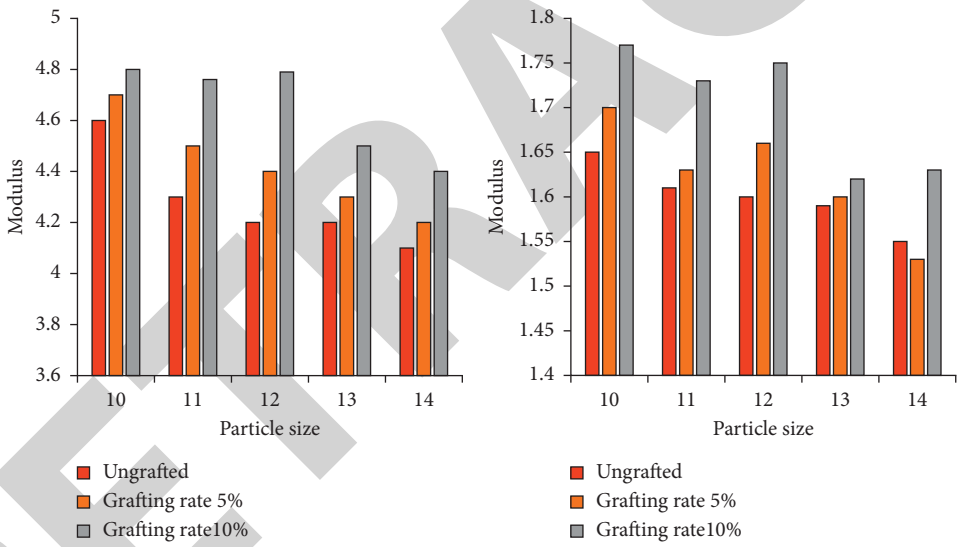

Figure 7: Schematic diagram of the relationship between composite material modulus and particle size.

mechanical energy of the composites, and the modified agglomerates indicate that the energy starts to decrease, allowing them to be more uniformly dispersed in the matrix, while improving the interfacial interaction with the matrix. From a macroscopic point of view, the modulus of elasticity is a measure of the magnitude of an object's resistance to elastic deformation, and at a microscopic level, it can be affected by any factor that can interfere with the strength of the check [35].

According to the data in Figure 7, it can be seen that Young's modulus and shear modulus of the composites have increased to different degrees after the modification treatment of nanoparticles, and according to the figure, it can be seen that the trend will increase with the increase of grafting rate, and at the same time, it appears that the performance of the composites will decrease with the increase of the direct drop of nanoparticles.

4.2. Single Cell Model Performance Analysis. According to the data in Figure 8, it can be seen that there is no significant difference in the effect of particle size on Young's modulus and shear modulus of the composites after grafting of nanoparticles, but when the grafting rate is changed to 5%, the change in the properties of the composites is very obvious, and according to the experimental data, the elastic modulus increases by more than 10% under the influence of this grafting rate [36].

4.3. Elastic Modulus of Composites and Matrix Material. In order to verify the validity of the theory, we used nanoparticle-reinforced composites as a research object to verify the correlation between the variation law of the effective shear modulus and the bulk modulus.

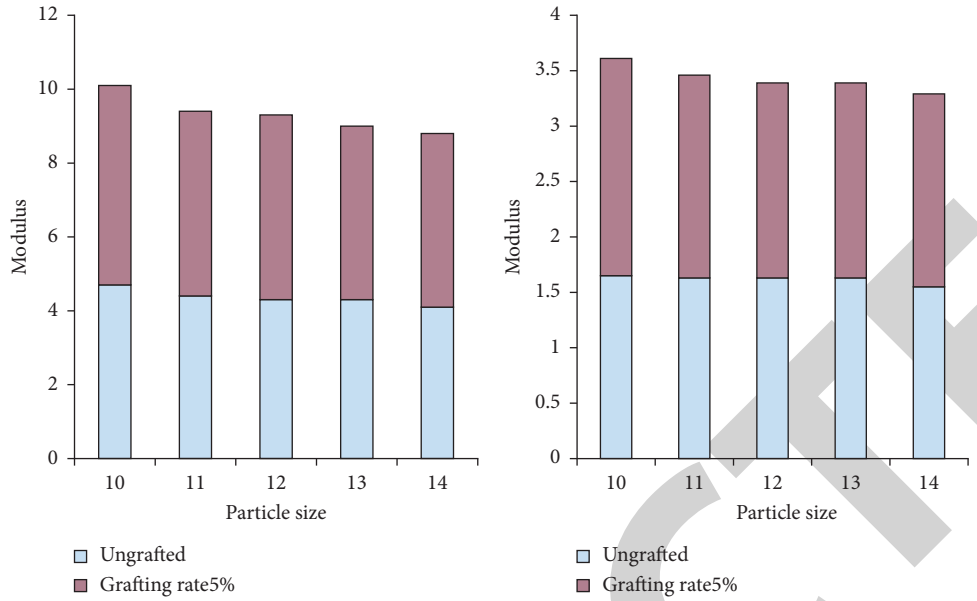

Figure 8: Schematic diagram of the relationship between composite shear modulus and particle size.

Figure 9: Schematic diagram of bulk modulus and shear modulus.

According to the data in Figure 9, we designed the ratio of the effective elastic modulus of the particle-reinforced composite to the effective modulus of the matrix material in the form of the above figure, and according to the derived data, it can be seen that the effective bulk modulus approaches the upper limit and then favors the lower limit when the volume of nanoparticles is increasing. It can also be observed that the variation pattern of the effective shear modulus shows a negative proportional relationship with the variation trend of the bulk modulus.

5. Conclusions

The purpose of this paper is to investigate the prediction of elastic modulus of nanoparticle-reinforced polymer matrix composites based on digital image processing and finite elements. Based on the experimental results, we found that the highest increase in tensile strength of the composites was about 8% and the highest increase in elastic modulus was 40% with the addition of nanoparticle materials, and the highest increase in tensile strength was 18% and the highest increase in elastic modulus was 50% with the addition of CNFs. In the experimental process of this paper, we mainly accomplished the following works:

(1) Based on the previous studies, we derived the calculation equation of nanoparticle-reinforced polymer matrix composites by combining the laws such as linear variation of interfacial materials and briefly discussed the relationship between the diameter and volume of nanoparticles.

(2) The correlation between the effective elastic modulus of the particle-reinforced composite and the effective modulus of the matrix material was experimentally investigated, and it was found that the effective bulk modulus would first approach the upper limit and then deviate to the lower limit when the volume of nanoparticles kept increasing, while the change pattern of the effective shear modulus showed a negative proportional relationship with the change trend of the bulk modulus.

(3) The increase of grafting rate will lead to the trend of increasing Young's modulus and shear modulus, and at the same time, the performance of the composite will decrease with the increase of nanoparticle direct drop. However, there are still many shortcomings in the process of exploration:

(i) The materials studied in this paper are isotropic materials with wired elastic mechanical properties, but this is not the case for the materials that appear in the actual processing

(ii) There are many deviations in the production and processing of composite materials that are difficult to detect with the naked eye, which are important factors in the performance of particle-reinforced composites, but they are not considered in this paper

(iii) The deformation factor and anisotropy of the composite materials are not taken into account in the experimental investigation, resulting in a certain degree of bias in the data obtained

Data Availability

No data were used to support this study.

Conflicts of Interest

The authors declare that there are no conflicts of interest regarding the publication of this article.

References

[1] Bo Gao, N. Xu, and P. Xing, "Shock wave induced nanocrystallization during the high current pulsed electron beam process and its effect on mechanical properties," *Materials Letters*, vol. 237, no. 15, pp. 180–184, 2019.

[2] Y. Zhang, Y. Li, and C. Bai, "Microstructure and oxidation behavior of Si-MoSi 2 functionally graded coating on Mo substrate," *Ceramics International*, vol. 43, no. 8, pp. 6250–6256, 2017.

[3] J. G. A. BarbedoBarbedo, "A novel algorithm for semi-automatic segmentation of plant leaf disease symptoms using digital image processing," *Tropical Plant Pathology*, vol. 41, no. 4, pp. 210–224, 2016.

[4] I. Stachiv, C. Y. Kuo, T. H. Fang, and V. Mortet, "Simultaneous determination of the residual stress, elastic modulus, density and thickness of ultrathin film utilizing vibrating doubly clamped micro-/nanobeams," *AIP Advances*, vol. 6, no. 4, Article ID 045005, 2016.

[5] R. A. Hawileh, J. A. Abdalla, S. S. Hasan, M. B. Ziyada, and A. Abu-Obeidah, "Models for predicting elastic modulus and tensile strength of carbon, basalt and hybrid carbon-basalt FRP laminates at elevated temperatures," *Construction and Building Materials*, vol. 114, no. jul.1, pp. 364–373, 2016.

[6] M. Nedeljković, B. Šavija, Y. Zuo, M. Luković, and G. Ye, "Effect of natural carbonation on the pore structure and elastic modulus of the alkali-activated fly ash and slag pastes," *Construction and Building Materials*, vol. 161, no. 10, pp. 687–704, 2018.

[7] W. Xu, M. Jia, Z. Zhu, M. Liu, D. Lei, and X. Gou, "n-Phase micromechanical framework for the conductivity and elastic modulus of particulate composites: design to micro-encapsulated phase change materials (MPCMs)-cementitious composites," *Materials & Design*, vol. 145, pp. 108–115, 2018.

[8] M. Z. Wei, J. Shi, Y. J. Ma, Z. Cao, and X. Meng, "The ultra-high enhancement of hardness and elastic modulus in Ag/Nb multilayers," *Materials Science and Engineering A*, vol. 651, no. 10, pp. 155–159, 2016.

[9] X. Tan, H. Konietzky, and W. Chen, "Numerical simulation of heterogeneous rock using discrete element model based on digital image processing," *Rock Mechanics and Rock Engineering*, vol. 49, no. 12, pp. 4957–4964, 2016.

[10] M. L. Xia, L. Wang, Z. X. Yang, and Hz Chen, "High-throughput screening of high Monascus pigment-producing strain based on digital image processing," *Journal of Industrial Microbiology and Biotechnology*, vol. 43, no. 4, pp. 451–461, 2016.

[11] E. M. Golafshani and A. Behnood, "Application of soft computing methods for predicting the elastic modulus of recycled aggregate concrete," *Journal of Cleaner Production*, vol. 176, no. 1, pp. 1163–1176, 2018.

[12] M. Gao, J. Zhao, S. W Li, and Zq Qiu, "Theoretical model of the equivalent elastic modulus of a cobblestone-soil matrix for TBM tunneling," *Tunnelling and Underground Space Technology*, vol. 54, no. Apr, pp. 117–122, 2016.

[13] P. Shan and X. Lai, "Mesoscopic structure PFC~2D model of soil rock mixture based on digital image," *Journal of Visual Communication and Image Representation*, vol. 58, pp. 407–415, 2019.

[14] R. J. Gaymans, J. Tijssen, S. Harkema, and A. Bantjes, "Elastic modulus in the crystalline region of poly(p-phenylene terephthalamide)," *Polymer*, vol. 17, no. 6, pp. 517-518, 1976.

[15] A. P. Chrysafi, N. Athanasopoulos, and N. J. Siakavellas, "Damage detection on composite materials with active thermography and digital image processing," *International Journal of Thermal Sciences*, vol. 116, pp. 242–253, 2017.

[16] V. Subramanian, E. E. Wolf, and P. V. Kamat, "Influence of metal/metal ion concentration on the photocatalytic activity of TiO2−Au composite nanoparticles," *Langmuir*, vol. 19, no. 2, pp. 469–474, 2003.

[17] P. Shan, "Image segmentation method based on K-mean algorithm," *EURASIP Journal on Image and Video Processing*, vol. 2018, no. 1, p. 81, 2018.

[18] U. K. Ghosh, K. K. Naik, and M. P. Kesari, "Digital image processing of multispectral ASTER imagery for delineation of alteration and related clay minerals in Sakoli belt: Maharashtra - a case study," *Journal of the Geological Society of India*, vol. 88, no. 4, pp. 464–470, 2016.

[19] E. Y. Kalafi, W. B. Tan, C. Town, and S. K Dhillon, "Automated identification of Monogeneans using digital image processing and K-nearest neighbour approaches," *BMC Bioinformatics*, vol. 17, no. 19, pp. 259–266, 2016.

[20] K. Schulze, S. M. Zehnder, J. Urueña, T. Bhattacharjee, W. Sawyer, and T. Angelini, "Elastic modulus and hydraulic permeability of MDCK monolayers," *Journal of Biomechanics*, vol. 53, pp. 210–213, 2017.

[21] J. Yang, C. Wang, B. Jiang, H. Meng, and Q. Meng, "Visual perception enabled industry intelligence: state of the art, challenges and prospects," *IEEE Transactions on Industrial Informatics*, vol. 17, no. 3, pp. 2204–2219, 2021.

[22] A. Abvabi, J. Mendiguren, A. Kupke, B. Rolfe, and M. Weiss, "Evolution of elastic modulus in roll forming," *International Journal of Material Forming*, vol. 10, no. 3, pp. 463–471, 2017.

[23] W. Zhao, J. L. Cheng, S. D. Feng, G. Li, and R. Liu, "Intrinsic correlation between elastic modulus and atomic bond stiffness in metallic glasses," *Materials Letters*, vol. 175, no. 15, pp. 227–230, 2016.

[24] X. Dai, X. Zhang, M. Xu et al., "Synergistic effects of elastic modulus and surface topology of Ti-based implants on early osseointegration," *RSC Advances*, vol. 6, no. 49, pp. 43685–43696, 2016.

[25] B. P. Binks, H. Kellay, and J. Meunier, "Bending elastic modulus of monolayers at oil-water interfaces," *Thin Solid Films*, vol. 210, no. 1, pp. 118–120, 1992.

[26] H. Chen, D. L. FanFan, L. FangFang et al., "Particle swarm optimization algorithm with mutation operator for particle filter noise reduction in mechanical fault diagnosis," *International Journal of Pattern Recognition and Artificial Intelligence*, vol. 34, no. 10, Article ID 2058012, 2020.

[27] C. Hu, "Comment on "Elastic modulus of a chemically bonded phosphate ceramic formulated with low-grade magnesium oxide determined by Nanoindentation"," *Ceramics International*, vol. 42, no. 2, pp. 3720-3721, 2016.

[28] M. Pianigiani, R. Kirchner, E. Sovernigo, A. Pozzato, M. Tormen, and H. Schift, "Effect of nanoimprint on the elastic modulus of PMMA: comparison between standard and ultrafast thermal NIL," *Microelectronic Engineering*, vol. 155, pp. 85–91, 2016.

[29] A. P. Luz, T. M. Souza, C. Pagliosa, M. Brito, and V. Pandolfelli, "In situ hot elastic modulus evolution of MgO-C refractories containing Al, Si or Al-Mg antioxidants," *Ceramics International*, vol. 42, no. 8, pp. 9836–9843, 2016.

[30] Y. Wu, Z. Ge, and Y. Luo, "Properties and application of a novel type of glycidyl azide polymer modified double-base spherical powders," *Journal of Thermal Analysis and Calorimetry*, vol. 124, no. 1, pp. 107–115, 2016.

[31] B. Mishra, A. Chaudhry, and V. Mittal, "Development of polymer-based composite coatings for the gas exploration industry: polyoxometalate doped conducting polymer based self-healing pigment for polymer coatings," *Materials Science Forum*, vol. 879, no. 1, pp. 60–65, 2016.

[32] P. L. Qin, G. Yang, Z. W. Ren et al., "Stable and efficient organo-metal halide hybrid perovskite solar cells via π-conjugated lewis base polymer induced trap passivation and charge extraction," *Advanced Materials*, vol. 30, no. 12, Article ID 1706126, 2018.

[33] B. Novianita, L. Hendarmin, and Y. Anggraeni, "The characterization of tomato juice patch as dental bleaching with hpmc-pvp combination polymer base," *Asian Journal of Microbiology, Biotechnology and Environmental Sciences*, vol. 22, no. 2, pp. 297–302, 2021.

[34] N. Ahmed, M. S. Alam, and M. A. Salam, "Experimental analysis of drilling fluid prepared by mixing iron (III) oxide nanoparticles with a KCl-Glycol-PHPA polymer-based mud used in drilling operation," *Journal of Petroleum Exploration and Production Technology*, vol. 10, no. 8, pp. 3389–3397, 2020.

[35] F. K. Soomro, S. Q. Memon, N. Memon, and M. Y. Khuhawar, "A new Schiff's base polymer for remediation of phenol, 2-chlorophenol and 2,4-dichlorophenol from contaminated aqueous systems," *Polymer Bulletin*, vol. 77, no. 5, pp. 2367–2383, 2020.

[36] W. Hu, Q. Nie, B. Huang et al., "Mechanical property and microstructure characteristics of geopolymer stabilized aggregate base," *Construction and Building Materials*, vol. 191, no. 10, pp. 1120–1127, 2018.